Physics Letters A 384 (2020) 126850

Contents lists available at ScienceDirect

Physics Letters A

www.elsevier.com/locate/pla

Magnetoexcitons in monolayer transition-metal dichalcogenides

Anastasia Spiridonova [a,b,*]

[a] The Graduate School and University Center, The City University of New York, New York, NY 10016, USA
[b] New York City College of Technology, The City University of New York, Brooklyn, NY 11201, USA

ARTICLE INFO

Article history:
Received 13 June 2020
Received in revised form 18 August 2020
Accepted 27 August 2020
Available online 31 August 2020
Communicated by L. Ghivelder

Keywords:
Binding energy
Excited states
Excitons
Magnetoexcitons
Diamagnetic shift
Transition-metal dichalcogenides

ABSTRACT

We study the magnetoexciton Rydberg states in MoS_2, $MoSe_2$, WS_2, and WSe_2 monolayers encapsulated by hexagonal boron nitride. Excitons in the magnetic field are described in the framework of the nonrelativistic potential model. We use the Rytova-Keldysh potential to calculate the energies of the magnetoexcitons. Our calculations use as inputs the effective masses of electron and hole obtained in the framework of the density functional theory. The binding energies of A and B magnetoexcitons are calculated by numerical integration of the Schrödinger equation. We report the energy contribution from the magnetic field to the binding energy and its dependence on the magnetic field. The diamagnetic coefficients are calculated. The reasonable agreement for diamagnetic coefficients and experimental data is obtained.

Transition-metal dichalcogenides (TMDCs) monolayers currently are extensively studied due to their remarkable properties that can be used in electronics. The breakdown of the inversion symmetry leads to the formation of a direct gap at two nonequivalent points K and K' of the Brillouin zone [1–3]. The two-dimensional confinement leads to the reduced dielectric screening [4,5] and the formation of tightly bound Mott excitons with binding energies larger than exciton binding energies in bulk TMDCs [1]. Semiconductors with the direct gap have more efficient radiative recombination of an electron and hole that serves as base of LEDs and semiconductor lasers [6].

Excitons in semiconductors have been studied for decades. Elliot and Loudon [7] and Hasegawa and Howard [8] developed the theory of the Mott exciton in a strong magnetic field. Physics of excitons in the magnetic field is considered in Refs. [9,10]. Authors of Refs. [9,11,12] addressed physics of excitons in the magnetic field based on works [7,8] including extremely anisotropic semiconductors [11,12]. A comprehensive review of the studies and computations of few-body systems of electrons and holes in condensed matter physics is given in Ref. [13]. Edelstein et al. [14] numerically solved the Schrödinger equation for the exciton using a program called SLEIGN to find wavefunctions and the energies for the ground and several excited states. The Zeeman shift has been considered in Refs. [1,15,17–26], and the diamagnetic (DM) shift was addressed in Refs. [1,15,18–20,22–24,27–33]. The experimental values of the binding energies of the excitons in TMDCs monolayers are given in Refs. [15–20,22–27,32–39]. We cite these articles, but the recent literature on the subject is not limited by them.

In early publications [9–12,14,31], the electromagnetic interaction between the hole and electron was taken to be the Coulomb potential. In recent studies related to two-dimensional (2D) materials [13,15,16,18,20–22,29,33–37], the interaction forming the exciton is taken to be the Rytova-Keldysh (RK) potential. The RK potential was first derived in Ref. [4] and then independently rederived in Ref. [5]. The RK potential describes the interaction of the two-body system by taking into account effects of the dielectric environment and the 2D confinement.

The problem of finding the dependence of the magnetoexciton binding energy on the magnetic field for excitons in TMDCs monolayers has been addressed before in Refs. [14,15,18,20–24,27–29,31]. To find the effect of the magnetic field on the exciton binding energy for the A exciton, in Refs. [15,18,22,27,33,36,43], the appropriate RK potential was used, but the magnetic field was treated as a small perturbation. This approach works well for excitons in states $1s$ and $2s$ even in the strong magnetic field. In the above works, for states $3s$ and $4s$, the approach of treating magnetic field as the small perturbations works well only at magnitudes such as $B \sim 5 - 15$ T. For s states, starting from $3s$ state, the quadratic dependence of the magnetoexciton binding energy

* Correspondence to: The Graduate School and University Center, The City University of New York, New York, NY 10016, USA.
E-mail address: aspiridonova@gradcenter.cuny.edu.

https://doi.org/10.1016/j.physleta.2020.126850
0375-9601/

on the magnetic field transforms into the linear dependence. According to Ref. [20], for states 3*s* and 4*s*, the region between 15 T and 31 T is an intermediate region where the quadratic dependence on the magnetic field transforms into the linear dependence. Treating magnetic field as the small perturbation works when the energy contribution from the magnetic field is small compared to energy gaps between states. This will be discussed below. A different approach to address the dependence of the binding energy on the magnetic field is presented in Ref. [22], where authors developed the model such that the Schrödinger equation with the magnetic field and the RK potential is solved numerically and compared the results of calculations with their experimental findings. Another approach is presented in Ref. [29], where stochastic variation method (SVM) is used to calculate the binding energy of the exciton at different magnetic field values. Following Ref. [29], we also do not take into account the Zeeman term.

In the present work we study the dependence of the binding energy for states 1*s*, 2*s*, 3*s*, and 4*s* on the magnetic field for direct *A* and *B* magnetoexcitons in the monolayer of TMDCs materials by numerical integration of the Schrödinger equation for the 2D exciton in the magnetic field using the Rytova-Keldysh potential. Excitons in the magnetic field are described in the framework of the nonrelativistic potential model. In our calculation, there are no fitting of parameters, and as input parameters we use the polarizability, χ_{2D}, effective masses for the electron, m_e, and hole, m_h, that are inputted as the reduced exciton mass, $\mu = \frac{m_e m_h}{m_e+m_h}$, and the layer thickness, h, which defines the screening length of the interaction of charged particles in 2D materials. We report the energy contribution from the magnetic field to the binding energy of *A* and *B* magnetoexcitons for states 1*s*, 2*s*, 3*s*, and 4*s* and the diamagnetic coefficients for states 1*s* and 2*s* in monolayers of WSe_2, WS_2, $MoSe_2$, and MoS_2.

The theoretical framework of considering the Zeeman and diamagnetic shifts, when contribution to the binding energy from magnetic field is small, is following. According to Ref. [31], the magnetoexciton binding energy, $E(B)$, for *A* and *B* excitons can be expanded in Taylor series as:

$$E(B) = E_0 + \gamma_1 B + \gamma_2 B^2 + ... \tag{1}$$

In Eq. (1) E_0 is the exciton binding energy in the absence of the magnetic field, and the terms $\gamma_1 B$ and $\gamma_2 B^2$ are identified as the valley Zeeman shift and diamagnetic shift, respectively. The valley Zeeman shift contribution to the binding energy is identified as $\gamma_1 B = -\mu_B g B$, where g is g-factor and μ_B is Bohr magneton [19,23]. The diamagnetic shift contribution to the binding energy is identified as $\gamma_2 B^2 = \frac{e^2 B^2}{8\mu}\langle r^2\rangle$ [18,27], where μ is the exciton reduced mass, e is the charge of the electron, and $\langle r^2\rangle$ is the expectation value of r^2 over the exciton envelope wave function. γ_2 is called the diamagnetic coefficient, σ. The decomposition of the magnetoexciton energy given in Eq. (1) is applicable when $E_0 > |E(B) - E_0|$. When $E_0 \sim |E(B) - E_0|$, the decomposition is no longer applicable and needs the consideration of the next terms in the Taylor series.

In literature [15,18,22,24,27], experimentally the valley Zeeman shift is defined as the energy difference between excitons located at Dirac points K and K', $-g\mu_B B = E(K) - E(K')$. Experimentally the energy contribution from the diamagnetic shift is defined as the average transition energy of each exciton state between points K and K', $\sigma B^2 = \frac{E(K)+E(K')}{2}$ [15,18,20,23,27]. The diamagnetic coefficient extracted from experimental data can be used to determine exciton masses, radius, and dielectric properties of a material [15,18,20,22,27].

Let us present the theoretical framework. We start with the Hamiltonian for the electron-hole system. The Hamiltonian has the following form [40]:

$$H = \frac{1}{2m_e}(-i\hbar\nabla_e + e\boldsymbol{A}_e)^2 + \frac{1}{2m_h}(-i\hbar\nabla_h - e\boldsymbol{A}_h)^2 + V(\boldsymbol{r}_e - \boldsymbol{r}_h). \tag{2}$$

In the Hamiltonian (2) $\boldsymbol{A}$ is the vector potential such that $\boldsymbol{B} = \nabla \times \boldsymbol{A}$, $V(\boldsymbol{r}_e - \boldsymbol{r}_h)$ is the central electron-hole interaction potential, and $\boldsymbol{r}_e$ and $\boldsymbol{r}_h$ are coordinates of the electron and hole, respectively. For the 2D system the appropriate potential is the Rytova-Keldysh potential that has the form [4,5]:

$$V(\boldsymbol{r}) = -\frac{\pi k e^2}{(\varepsilon_1+\varepsilon_2)\rho_0}\left[H_0\left(\frac{r}{\rho_0}\right) - Y_0\left(\frac{r}{\rho_0}\right)\right]. \tag{3}$$

In Eq. (3) $H_0(x)$ and $Y_0(x)$ are Struve and Bessel functions of the second kind of order $\nu = 0$, respectively, $\rho_0 = \frac{2\pi\chi_{2D}}{\kappa}$ is the screening length, r is the distance between an electron and a hole, and $k \equiv \frac{1}{4\pi\varepsilon_0}$, where ε_0 is the permittivity of free space.

Following Refs. [7,9–12,40], we rewrite the Hamiltonian (2) using the standard change of coordinate to the center-of-mass, $\boldsymbol{R} = \frac{m_e\boldsymbol{r}_e - m_h\boldsymbol{r}_h}{M}$, and the relative motion, $\boldsymbol{r} = \boldsymbol{r}_e - \boldsymbol{r}_h$, coordinates, where the total mass of the system is $M = m_e + m_h$, and by choosing the symmetric gauge, $\boldsymbol{A}_{e,h} = \frac{1}{2}\boldsymbol{B}\times\boldsymbol{r}_{e,h}$, and by considering the magnetic field pointing in z-direction that is perpendicular to the monolayer where the exciton is located.

Following Ref. [9,10,40] we use an operator $\hat{\boldsymbol{P}}$ to find the wave function for the two-body system in the magnetic field. The operator $\hat{\boldsymbol{P}}$ is defined as:

$$\hat{\boldsymbol{P}} = -i\hbar\nabla_{\boldsymbol{R}} - \frac{e}{2}(\boldsymbol{B}\times\boldsymbol{r}). \tag{4}$$

Since $\hat{\boldsymbol{P}}$ commutes with the Hamiltonian, $[H, \hat{\boldsymbol{P}}] = 0$, $\hat{\boldsymbol{P}}$ and H have the same eigenfunction. As a result, one can write, the wave function for the exciton in the magnetic field as [9,10]:

$$\psi(\boldsymbol{R},\boldsymbol{r}) = e^{\left[\frac{i}{\hbar}\boldsymbol{R}\cdot(\boldsymbol{P}+\frac{e}{2}\boldsymbol{B}\times\boldsymbol{r})\right]}e^{\frac{1}{2}i\gamma\boldsymbol{r}\cdot\boldsymbol{P}}\Theta(\boldsymbol{r}). \tag{5}$$

In Eq. (5) $\gamma = \frac{m_h - m_e}{m_h + m_e}$. After acting with the Hamiltonian on the wave function $\psi(\boldsymbol{R},\boldsymbol{r})$, the Schrödinger equation for the relative motion of the electron and hole takes the following form [10]:

$$\left[-\frac{\hbar^2}{2\mu}\frac{\partial^2}{\partial\boldsymbol{r}^2} - \frac{i\hbar e\gamma}{2\mu}(\boldsymbol{B}\times\boldsymbol{r})\cdot\frac{\partial}{\partial\boldsymbol{r}} + \frac{e^2}{8\mu}(\boldsymbol{B}\times\boldsymbol{r})^2 + V(\boldsymbol{r})\right]\Theta(\boldsymbol{r}) = E\Theta(\boldsymbol{r}). \tag{6}$$

In Eq. (6) the potential $V(\boldsymbol{r})$ is the RK potential given in Eq. (3). We consider the Rydberg optical states - 1*s*, 2*s*, 3*s*, and 4*s* states ($l = 0$, $m_l = 0$). Therefore, the term $(\boldsymbol{B}\times\boldsymbol{r})\cdot\frac{\partial}{\partial\boldsymbol{r}} = \frac{1}{2}\boldsymbol{B}\cdot\boldsymbol{L}$ is equal to 0. Finally, the radial Schrödinger equation that we numerically integrate to find the magnetoexciton binding energy of *s* states has the form [9,10]:

$$\left[-\frac{\hbar^2}{2\mu}\frac{\partial^2}{\partial\boldsymbol{r}^2} + \frac{e^2}{8\mu}(\boldsymbol{B}\times\boldsymbol{r})^2 + V(\boldsymbol{r})\right]\Theta(\boldsymbol{r}) = E\Theta(\boldsymbol{r}). \tag{7}$$

To find the binding energy of the direct exciton in TMDCs we use the code implemented in Ref. [41]. The code was modified in a way that the Schrödinger equation explicitly includes $\frac{e^2}{8\mu}(\boldsymbol{B}\times\boldsymbol{r})^2$ term. The latter allows us to numerically solve Eq. (7), which includes the contribution of magnetic field. The benefit of our approach is that we can obtain the eigenfunctions and eigenenergies of the

Table I
The comparison between binding energies, E_0, of the A exciton in WSe_2 that were determined for 1s, 2s, 3s, and 4s states using our approach with parameters from Ref. [15,27,43] and results reported in Ref. [15,27,43]. The binding energy is given in meV. To a very good precision, we reproduce known results.

State	Results of calculations					
	Ref. [15]	Present calculations with parameters from Ref. [15]	Ref. [27]	Present calculations with parameters from Ref. [27]	Ref. [43]	Present results with parameters from Ref. [43]
1s	172	172.38	161	161.47	294.6	294.62
2s	41	43.84	37	37.39		
3s	20	19.54	15.7	16.12		
4s	11	10.97				

Table II
The comparison of the binding energies, E_0, of A and B excitons in 1s state in TMDCs obtained using our approach with parameters given in Refs. [22,43] and energies reported in Refs. [22,43], respectively. The binding energy is given in meV.

TMDCs	The A exciton		The B exciton	
	Ref. [22]	Present calculations with parameters given in Ref. [22]	Ref. [43]	Present calculations with parameters given in Ref. [43]
WSe_2	167	161.45	477.37	477.7
WS_2	180	178.68	530.09	530.9
MoS_2	221	220.19	533.45	533.9
$MoSe_2$	231	231.96	485.22	485.3

magnetoexcitons for any value of the magnetic field. In our calculations, we do not have a linear term (the Zeeman shift) [42] in Eq. (1) since we consider s states for which $\boldsymbol{B} \cdot \boldsymbol{L} = 0$ and we do not consider spin - magnetic field interaction, $\boldsymbol{S} \cdot \boldsymbol{B} = 0$ [42]. Therefore, the energy contribution from the magnetic field to the binding energy that we calculate is the diamagnetic shift contribution in states 1s and 2s where Taylor series expansion of second order is applicable.

In contrast to our approach in Refs. [15,18,27], the analytical and numerical approach to finding the energy contribution from the diamagnetic shift to the magnetoexciton binding energy of the A exciton at the low magnetic field is to solve the Schrödinger equation without magnetic field and to treat the magnetic field as the small perturbation. In Ref. [22] authors developed the model for revealing exciton masses and dielectric properties of the monolayer semiconductors with high magnetic fields by solving numerically the corresponding Schrödinger equation with the RK potential, while in Ref. [15], the corresponding Hamiltonian was diagonalized to find the DM coefficients.

As a first step, we check out code by determining the binding energy for the A exciton in WSe_2 for 1s, 2s, 3s, and 4s states, when magnetic field is absent, with parameters given in Refs. [15,27,43]. Results of our calculations and for comparison the corresponding results from Refs. [15,27,43] are given in Table I. We also have determined 1s state binding energies of the A and B excitons in MoS_2, $MoSe_2$, WS_2, and WSe_2 monolayers, in the absence of magnetic field, using parameters from [22,43]. The results are given in Table II. Additionally, our calculations reproduce experimental results for 1s and 2s states given in Refs. [33,36,37] and difference of the energies between above states for $MoSe_2$ and MoS_2 reported in [32] with parameters they provide. We reproduce results obtained within the analytical approach of finding the binding energy of the exciton [44] where the binding energy of the Rydberg series is scaled as an energy ladder. The ground state binding energies in different TMDCs obtained using SVM [29] are reproduced too. In addition, we calculated the exciton binding energies at magnetic field values varying from 0 T to 30 T for 1s, 2s, 3s, and 4s in WSe_2 with parameters given in Refs. [15,27] and extracted the diamagnetic coefficient. Our results with good precision reproduce diamagnetic coefficients given in Ref. [27]. However, our calculations reproduce theoretical σ [15] for states 1s, 2s, and 3s with percentage difference between 0% and 10% and experimental σ [15] that has percentage difference higher than 25%. Based on the results in Tables I and II and the fact that we can reproduce the exciton binding energies in the absence of the magnetic field and approximately reproduce diamagnetic coefficients reported in literature, we conclude that our approach with high precision reproduces A and B excitons binding energies and changes of the binding energy due the magnetic field reported in literature.

Next step, we perform the calculation for A and B excitons with parameters given in literature and printed in Table III. We list following parameters in Table III with corresponding references: the exciton reduced mass, μ, the 2D material polarizability, χ_{2D}, and the layer thickness, h. For encapsulated by the hexagonal boron nitride (h-BN) TMDC monolayer, the dielectric constant is taken to be $\kappa_{h-\mathrm{BN}} = 4.89$ where $\kappa = \frac{\varepsilon_1+\varepsilon_2}{2}$ is the average dielectric constant of the surrounding material, and ε_1, ε_2 are dielectric constants of materials on both sides of the TMDC layer. For the A exciton two sets of parameters are given. In Table III the left and center sub-columns list combinations of parameters for each material that give the highest and lowest A exciton binding energies, $E_{A_{\mathrm{high/low}}}(B)$, respectively. Since we list combinations of parameters that give the highest/lowest values for the binding energies, we can calculate ranges for the A exciton binding energies and the energy contribution from the magnetic field to the binding energy. Parameters for the B exciton to find $E_B(B)$ are listed in the right sub-column in Table III. We perform calculations for the A and B excitons in states 1s, 2s, 3s, and 4s (Rydberg optical states) when magnetic field varies from 0 T to 31 T. We take this range because of data availability in literature. We calculate the energy contribution $\Delta E_{A_{\mathrm{high/low}}}(B)$ to the magnetoexciton binding energy, $E_{A_{\mathrm{high/low}}}(B)$, from the magnetic field, described later on.

The results of our calculations for the exciton binding energies for the direct A and B excitons in MoS_2, $MoSe_2$, WS_2, and WSe_2 monolayers, when magnetic field is absent, $E_0 \equiv E_{A_{\mathrm{high/low}}}(0)$ and $E_0 \equiv E_B(0)$ for A and B excitons, respectively, for states 1s, 2s, 3s, and 4s are reported in Table IV. In Table IV, left and center sub-columns present the exciton binding energies with combinations of parameters that give $E_{A_{\mathrm{high/low}}}(B)$, respectively. The B exciton binding energies are reported in Table IV in the right sub-column. As can be seen based on Tables I, II, and IV, exciton binding energies of Rydberg states in WSe_2, WS_2, $MoSe_2$, and MoS_2 calculated with electron-hole masses obtained in the framework of the density functional theory do not match perfectly experimental results. In addition, the percentage different between binding energies we

Table III
Parameters for the A and B excitons. Parameters for the A exciton reprinted here from Ref. [41] for MoS_2, $MoSe_2$, WS_2, and WSe_2. For the A exciton for each material two values of μ and χ_{2D} are given. The values in the left sub-column list combination of parameters that give the highest exciton binding energy, $E_{A_{\text{high}}}(B)$. The values in the center sub-column list combination of parameters that give the lowest exciton binding energy, $E_{A_{\text{low}}}(B)$. The right sub-column lists parameters for the B exciton that are reprinted from Ref. [43,45]. The average dielectric constant, $\kappa = \frac{\varepsilon_1+\varepsilon_2}{2} = 4.89$, is taken from Ref. [46]. κ is the same for all materials. μ is measured in units of electron mass, m_0. χ_{2D} and h are measured in Å.

Parameter	WSe_2			WS_2			$MoSe_2$			MoS_2		
	$E_{A_{\text{high}}}$	$E_{A_{\text{low}}}$	E_B	$E_{A_{\text{high}}}$	$E_{A_{\text{low}}}$	E_B	$E_{A_{\text{high}}}$	$E_{A_{\text{low}}}$	E_B	$E_{A_{\text{high}}}$	$E_{A_{\text{low}}}$	E_B
μ (m_0)	0.27	0.15	0.16	0.23	0.15	0.15	0.31	0.27	0.29	0.28	0.16	0.24
χ_{2D} (Å)	7.18	7.571	7.518	6.03	6.393	6.06	8.23	8.461	8.23	6.60	7.112	6.6
h (Å)	6.575			6.219			6.527			6.18		

Table IV
Calculated binding energies, E_0, of A and B excitons in MoS_2, $MoSe_2$, WS_2, and WSe_2 monolayers for 1s, 2s, 3s, and 4s states. The exciton binding energies are calculated with parameters given in Table III. E_0 is given in meV.

State	WSe_2			WS_2			$MoSe_2$			MoS_2		
	$E_{A_{\text{high}}}$	$E_{A_{\text{low}}}$	E_B	$E_{A_{\text{high}}}$	$E_{A_{\text{low}}}$	E_B	$E_{A_{\text{high}}}$	$E_{A_{\text{low}}}$	E_B	$E_{A_{\text{high}}}$	$E_{A_{\text{low}}}$	E_B
1s	172.21	124.16	133.34	173.33	133.95	138.36	170.98	158.02	165.09	183.03	132.31	170.39
2s	41.34	25.93	28.09	38.11	26.80	27.43	44.11	39.60	41.75	43.39	27.65	38.89
3s	18.04	10.82	11.75	16.16	11.04	11.27	19.77	17.55	18.57	18.85	11.54	16.69
4s	10.03	5.89	6.41	8.86	5.98	6.09	11.13	9.83	10.41	10.46	6.28	9.2

report in Table IV for tungsten based materials (WSe_2 and WS_2) varies between about 0.7% and up to 12%. For molybdenum based materials ($MoSe_2$ and MoS_2) the percentage difference of $E_{A_{\text{high}}}$ and E_B varies between 1.7% and 11%. For $E_{A_{\text{low}}}$ percentage difference varies between 18% and 44%. These results demonstrate the sensitivity of the binding energies to the input parameters used in our calculations. It is worth noticing that, by using as inputs the parameters obtained by fitting of the experimental values of binding energy, we exactly reproduce the available experimental values of binding energies for TMDC materials. However, our goal is to investigate the energy contribution from the magnetic field to the binding energy using parameters obtained in theoretical framework rather than investigating the effect of the magnetic field on the binding energy with parameters obtained by fitting experimental data.

In addition to reporting the binding energies of the excitons in the absence of the magnetic field, we report the energy contribution from the magnetic field to the binding energy, $\Delta E(B)$, and extract diamagnetic coefficients, σ, for states 1s and 2s from the energy contribution for A and B magnetoexcitons. The energy contribution from the magnetic field to the binding energy for states 1s, 2s, 3s, and 4s in MoS_2, $MoSe_2$, WS_2, and WSe_2 monolayers is found in the following way:

$$\Delta E(B) = E_0 - E(B). \tag{8}$$

The results for WSe_2 and $MoSe_2$ are presented in Figs. 1 and 2, respectively. In these Figures, we adopt notations where the solid and open markers indicate $\Delta E_{A_{\text{high}}}(B)$ and $\Delta E_{A_{\text{low}}}(B)$ for A magnetoexcitons, respectively. A solid green star marker indicates ΔE_B for B magnetoexcitons. As mentioned before, it is highly likely that the true value of the energy contribution from magnetic field to the A magnetoexciton binding energy lies in range between $\Delta E_{A_{\text{high}}}$ and $\Delta E_{A_{\text{low}}}$ that we report. Analysis of the results shows that the energy contribution from the magnetic field to the magnetoexciton binding energy depends on material parameters. The fact that the binding energy of magnetoexcitons is an increasing function of μ and a decreasing function of χ_{2D} coincides with previously reported calculations for excitons [41].

We report the energy dependence of magnetoexcitons on the magnetic field only for WSe_2 and $MoSe_2$. The dependence of the binding energy of A and B magnetoexcitons in WS_2 and MoS_2 monolayers on the magnetic field has similar behavior as the magnetoexcitons in WSe_2. The energy contribution to the binding energy from the magnetic field in these three materials lies in the same range for each s state. However, for $MoSe_2$ the energy contribution from the magnetic field for state 1s is four times smaller and for state 2s is three times smaller than in the other three materials that we examined. Another distinct feature of $MoSe_2$ is that the exciton state energy becomes positive at higher magnetic field values than in other TMDCs we examined. It can be noted in Figs. 1 (c) and (d) and 2 (d) where the data is not given for the full range that we examined. The reason is following. For these magnetoexcitons the energy contribution from the magnetic field to the binding energy becomes of order of the binding energy of excitons in these states. In other words, at values of the magnetic field given in Table V the energy of a state becomes positive and exciton ionization occurs [47–50]. Physics of ionized excitons is out of the scope of this paper and will be addressed in future work.

We plot the energy contribution from the magnetic field to the binding energy versus B^2 to indicate the linear dependence on square of the magnetic field i.e., the quadratic dependence on the magnetic field. Based on results presented in Figs. 1 and 2, the quadratic dependence of the energy contribution from the magnetic field can be seen for states 1s and 2s for magnetic field ranging from 0 T to 31 T in Figs. 1(a) and 2(b), respectively, since for these states $E_0 \gg |E(B) - E_0|$. For states 3s and 4s in Figs. 1(c) and 2(d), respectively, the quadratic dependence of the energy contribution on the magnetic field is observable only at a few Tesla where for these states $E_0 \geq |E(B) - E_0|$. The energy contribution from the magnetic field departs from quadratic dependence when $E_0 \sim |E(B) - E_0|$. So, on one hand, based on results we present in Figs. 1 and 2, in state 1s the magnetic field has a little effect on the binding energy in all examined materials for the input parameters given in Table III. In state 2s the contribution to the binding energy is ten times bigger compared to ΔE in state 1s. On the other hand in states 3s and 4s the energy contribution from the magnetic field becomes on the order of the binding energy of the state.

According to our results, the contribution from the magnetic field to the binding energy of the B magnetoexciton in WSe_2 and WS_2 is similar to the contribution of the A magnetoexciton with the parameters that give the lowest binding energy. There is no such trend in molybdenum based dichalcogenides materials. These trends can be expected from examination of parameters given in Table III. Parameters for the B exciton in WSe_2 and WS_2 are very close to parameters of the A exciton that give the lowest binding energy.

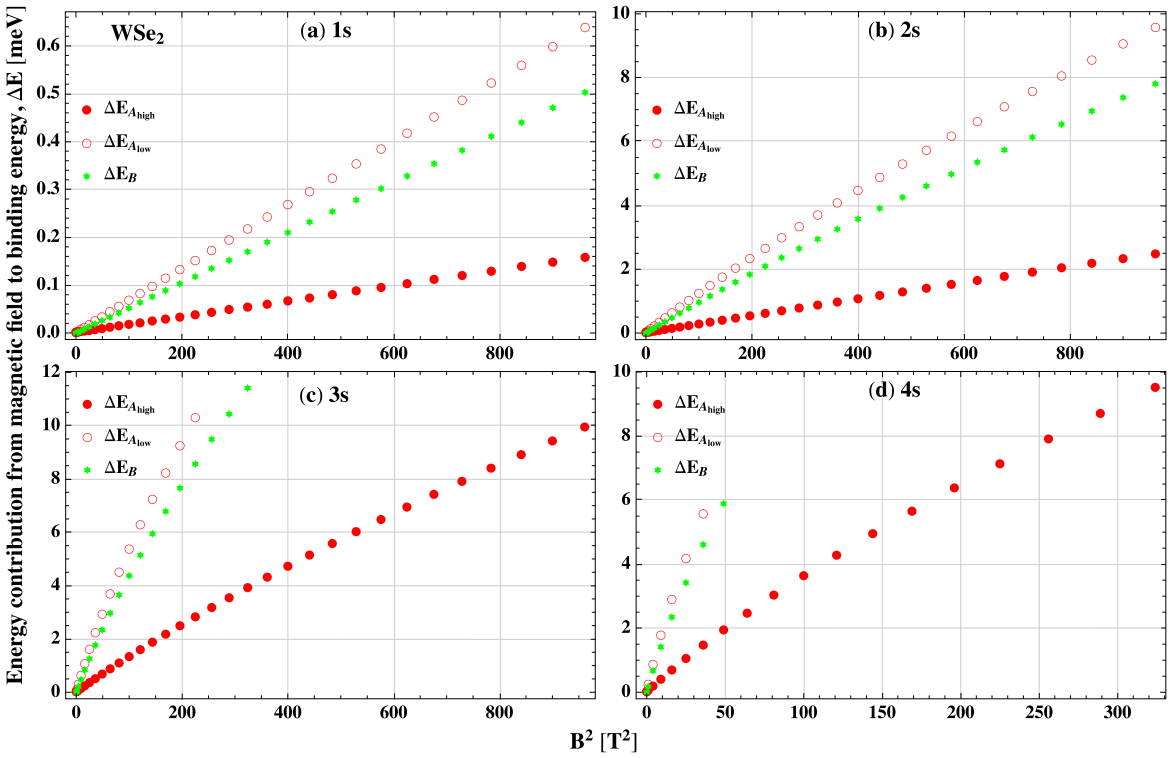

Fig. 1. The energy contribution from the magnetic field to the binding energy of the magnetoexciton versus B^2 for the states 1s, 2s, 3s, and 4s shown in (a), (b), (c) and (d), respectively. The calculations are performed for WSe_2. The energy contribution is given in meV. Open and solid markers correspond to $\Delta E_{A_{\text{low}}}(B)$ and $\Delta E_{A_{\text{high}}}(B)$ for the A exciton, respectively. The solid star marker corresponds to $\Delta E_B(B)$ for the B exciton. (For interpretation of the colors in the figure(s), the reader is referred to the web version of this article.)

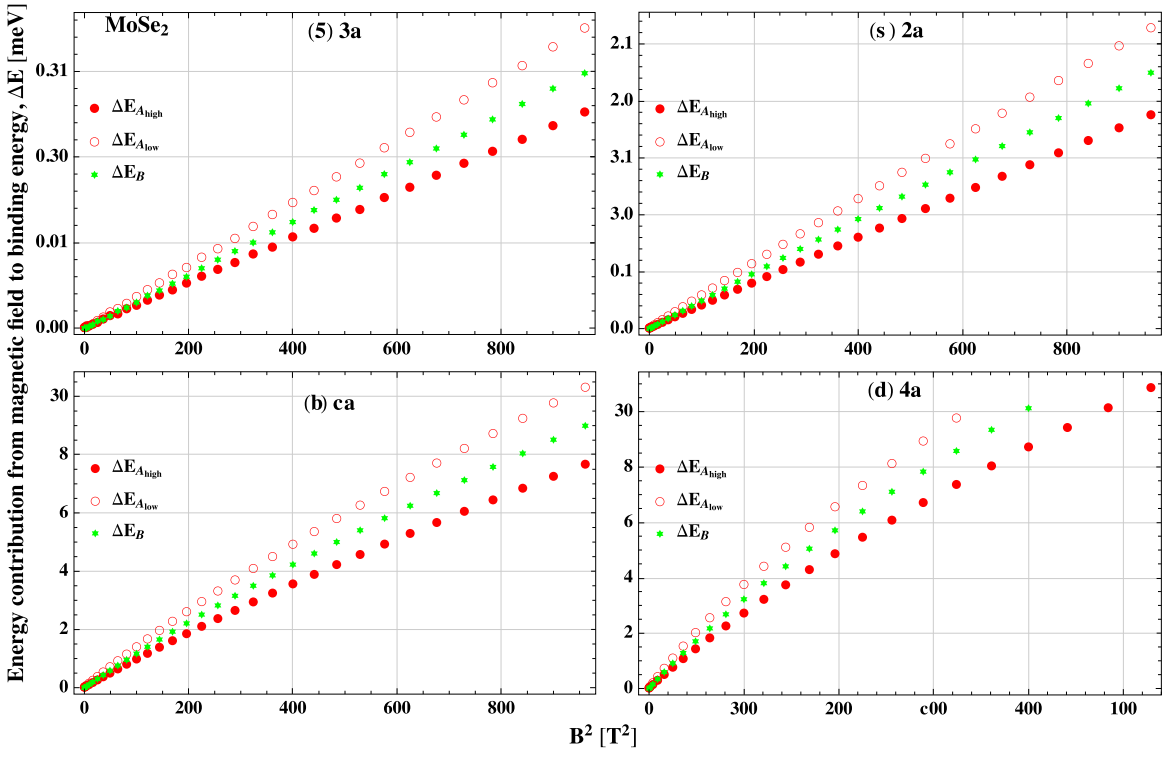

Fig. 2. The same as in Fig. 1. Calculations are performed for $MoSe_2$.

Table V
The magnetic field values at which the energy of the excitons' state $E_{A_{\text{low/high}}}$ and E_B becomes positive in MoS_2, $MoSe_2$, WS_2, and WSe_2 monolayers for $3s$ and $4s$ states.

State	Magnetic field value in T											
	WSe_2			WS_2			$MoSe_2$			MoS_2		
	$E_{A_{\text{high}}}$	$E_{A_{\text{low}}}$	E_B	$E_{A_{\text{high}}}$	$E_{A_{\text{low}}}$	E_B	$E_{A_{\text{high}}}$	$E_{A_{\text{low}}}$	E_B	$E_{A_{\text{high}}}$	$E_{A_{\text{low}}}$	E_B
3s		16	18		16	17					18	
4s	19	7	7	15	7	7	24	19	21	21	8	16

Table VI
The diamagnetic coefficients $\sigma_{A_{\text{high/low}}}$ for A exciton extracted from $\Delta E_{A_{\text{high/low}}}(B)$, and σ_B is extracted from $\Delta E_B(B)$. For WSe_2 σ_A from Refs. [15,27] are given. For WS_2 σ_A is given from Refs. [18,33]. Note in Ref. [33] measurements were taken on the same sample but at two different positions. No other experimental values of diamagnetic coefficient are available in literature. σ is measured in $\mu eV/T^2$.

State	WSe_2					WS_2					
	$\sigma_{A_{\text{high}}}$	$\sigma_{A_{\text{low}}}$	σ_B	σ_A [15]	σ_A [27]	$\sigma_{A_{\text{high}}}$	$\sigma_{A_{\text{low}}}$	σ_B	σ_A [18]	σ_A^{pos1} [33]	σ_A^{pos2} [33]
1s	0.16	0.66	0.57	0.24	0.31	0.21	0.60	0.61	0.32	0.58	1.2
2s	2.58	10.01	8.84	6.4	4.6	3.56	9.65	9.84		4.9	7.9
3s				27.3	22						
4s				53.7							

Table VII
The diamagnetic coefficients $\sigma_{A_{\text{high/low}}}$ for A exciton extracted from $\Delta E_{A_{\text{high/low}}}(B)$, and σ_B is extracted from $\Delta E_B(B)$. We could not find experimental or theoretical values of σ for excitons in $MoSe_2$ and MoS_2. σ is measured in $\mu eV/T^2$.

State	$MoSe_2$			MoS_2		
	$\sigma_{A_{\text{high}}}$	$\sigma_{A_{\text{low}}}$	σ_B	$\sigma_{A_{\text{high}}}$	$\sigma_{A_{\text{low}}}$	σ_B
1s	0.13	0.18	0.17	0.213	0.55	0.22
2s	1.96	2.76	2.55	3.56	8.64	3.50

We have performed calculations for the A exciton using two sets of parameters because of availability of lower and upper bounds on parameters in literature and to give better overview of the energy contribution from the magnetic field to the binding energy since majority of experimental data is available for the A exciton. The results we report for A excitons can be compared with experimental results. As far as we know, experimental results for the B exciton have been reported in Ref. [22]. Ref. [22] reports that for A and B excitons in MoS_2, B exciton in state $1s$ has slightly higher binding energy than A exciton in $2s$ state, and in $MoSe_2$ the A exciton in $2s$ state has slightly higher binding energy than the B exciton in $1s$ state. Our results do not show such trends.

In our calculations, since we do not have a linear term (the Zeeman shift), $\Delta E(B)$ that we calculate is the diamagnetic shift contribution to the binding energy, where Taylor series expansion of second order is applicable in states $1s$ and $2s$. The diamagnetic coefficients for A and B excitons extracted from our data for states $1s$ and $2s$ are reported in Table VI for WSe_2 and WS_2 and in Table VII for $MoSe_2$ and MoS_2. For comparison, in Table VI we give the diamagnetic coefficients reported in Refs. [15,27] for WSe_2 and from Refs. [18,33] for WS_2. According to Table VI, experimental results reported in literature fall in between $\sigma_{A_{\text{high}}}$ and $\sigma_{A_{\text{low}}}$ that we report. In addition, in contrast to results in literature, we observe that states $3s$ and $4s$ have the quadratic dependence on the magnetic field in TMDCs only at a few Tesla. So we do not report diamagnetic coefficients for the $3s$ and $4s$ states because $E_0 \sim |E(B) - E_0|$ and higher order terms in the Taylor series need to be taken into account. To the best of our knowledge, no experimental diamagnetic coefficients for B excitons are available in literature.

The diamagnetic coefficients we report are not always matching the coefficients reported in literature. However, this is the result of input parameters we used that are different from parameters obtained by fitting of data in the experimental works. The diamagnetic coefficient strongly depends on the parameters. Refs. [18,43,51,52] have shown that the exciton binding energy strongly depends on the dielectric constant of the encapsulating material. Smaller κ leads to higher value of the binding energy. It is worth mentioning that dielectric constant affects the exciton radius [18] and, therefore, affects σ. In addition, the excitons with lower μ have higher binding energy change with the magnetic field than excitons with large μ [29]. This can explain the large values of $\sigma_{A_{\text{low}}}$ for excitons in WSe_2, WS_2, and MoS_2.

In summary, we have examined the dependence of the binding energy of the direct A and B magnetoexcitons in TMDCs monolayer on the magnetic field using an exact numerical integration of the Schrödinger equation with the Rytova-Keldysh potential. We report $\Delta E_{A_{\text{high/low}}}$ for the A exciton and ΔE_B for the B exciton and diamagnetic coefficients for states $1s$ and $2s$ in monolayers of MoS_2, $MoSe_2$, WS_2, and WS_2. Previously reported values of σ_A [15,27] in WSe_2 fall between $\sigma_{A_{\text{high/low}}}$. According to our calculations, in states $3s$ and $4s$ the energy contribution from the magnetic field to the binding energy of magnetoexciton becomes comparable to the exciton binding energy in the absence of the magnetic field. Therefore, higher order terms in Taylor series need to be considered. In addition, in states $3s$ and $4s$ the magnetoexciton state energy becomes positive in the range between 6 T and 31 T. In states $3s$ and $4s$, because the energy contribution from the magnetic field to the binding energy is on order of the binding energy, extracting the diamagnetic coefficient may not be the best approach to analyze ΔE. Overall, our study demonstrates that experimental and other theoretical diamagnetic coefficients for A excitons given in literature for states $1s$ and $2s$ fall in the range that we report here when σ is extracted from the data calculated using input parameters obtained in the density functional theory. Our results can stimulate further experimental and theoretical studies of magnetoexcitons in TMDCs materials to achieve better agreement between results, exciton ionization, and can be used for the comparison with further experimental data.

CRediT authorship contribution statement

Anastasia Spiridonova: the writing of the manuscript, data acquisition, analysis, and calculations were performed by the author.
(Not a Co-author) Roman Ya. Kezerashvili: Funding Acquisition, Project Administration, Supervision.

Declaration of competing interest

The authors declare that they have no known competing financial interests or personal relationships that could have appeared to influence the work reported in this paper.

Acknowledgements

A.S. gratefully acknowledges helpful discussions with R. Ya. Kezerashvili, M. N. Brunettii O. L. Berman, and Yu. E. Lozovik. This work is supported by the U.S. Department of Defense under Grant No. W911NF1810433.

References

[1] M. Van der Donck, M. Zarenia, F.M. Peeters, Phys. Rev. B 97 (2018) 081109(R).
[2] J.A. Wilson, A.D. Yoffe, Adv. Phys. 18 (1969) 193–335.
[3] L. Britnell, R. Ribeiro, A. Eckmann, R. Jalil, B. Belle, A. Mishchenko, Y.-J. Kim, R. Gorbachev, T. Georgiou, S. Morozov, Science 340 (2013) 1311.
[4] N.S. Rytova, Proc. Mosc. State Univ., Phys. Astron. 3 (1967) 30.
[5] L.V. Keldysh, JETP Lett. 29 (1979) 658.
[6] P. Avouris, T. Heinz, T. Low (Eds.), 2D Materials: Properties and Devices, Cambridge University Press, Cambridge, 2017.
[7] R.J. Elliott, R. Loudon, J. Phys. Chem. Solids 15 (1960) 196.
[8] H. Hasegawa, R.E. Howard, J. Phys. Chem. Solids 21 (1961) 179.
[9] L.P. GorKov, I.E. Dzualoshinskii, Zh. Eksp. Teor. Fiz. 53 (1967) 717722.
[10] Yu.E. Lozovick, A.M. Ruvinsky, Phys. Lett. A 227 (1997) 271284.
[11] M. Shinada, S. Sugano, J. Phys. Soc. Jpn. 20 (1965) 1274.
[12] O. Akimoto, H. Hasegawa, J. Phys. Soc. Jpn. 22 (1967).
[13] R.Ya. Kezerashvili, Few-Body Syst. 60 (2019) 52.
[14] W. Edelstein, H.N. Spector, R. Marasas, Phys. Rev. B 39 (1989) 7697.
[15] E. Liu, J. Baren, T. Taniguchi, K. Watanabe, Y.-C. Chang, C.H. Lui, Phys. Rev. B 99 (2019) 205420.
[16] A. Chernikov, T.C. Berkelbach, H.M. Hill, et al., Phys. Rev. Lett. 113 (2014) 076802.
[17] M. Koperski, M.R. Molas, A. Arora, K. Nogajewski, M. Bartos, J. Wyzula, D. Vaclavkova, P. Kossacki, M. Potemski, 2D Mater. 6 (2019) 015001.
[18] A. Stier, K. McCreary, B. Jonker, et al., Nat. Commun. 7 (2016) 10643.
[19] G. Aivazian, Z. Gong, A. Jones, et al., Nat. Phys. 11 (2015) 148–152.
[20] S.Y. Chen, Z. Lu, T. Goldstein, et al., Nano Lett. 19 (2019) 2464–2471.
[21] D.V. Rybkovskiy, I.C. Gerber, M.V. Durnev, Phys. Rev. B 96 (2017) 155406.
[22] M. Goryca, J. Li, A.V. Stier, et al., Nat. Commun. 10 (2019) 4172.
[23] D. MacNeill, C. Heikes, K.F. Mak, et al., Phys. Rev. Lett. 114 (2015) 037401.
[24] G. Plechinger, P. Nagler, A. Arora, et al., Nano Lett. 16 (12) (2016) 7899–7904.
[25] A. Srivastava, M. Sidler, A. Allain, et al., Nat. Phys. 11 (2015) 141–147.
[26] Y. Li, J. Ludwig, T. Low, A. Chernikov, et al., Phys. Rev. Lett. 113 (2014) 266804.
[27] A.V. Stier, N.P. Wilson, K.A. Velizhanin, J. Kono, X. Xu, S.A. Crooker, Phys. Rev. Lett. 120 (2018) 057405.
[28] F. Luckert, M.V. Yakushev, et al., Appl. Phys. Lett. 97 (2010) 162101.
[29] M. Van der Donck, M. Zarenia, F.M. Peeters, Phys. Rev. B 97 (2018) 195408.
[30] B.K. Choi, Y. Kim, J.D. Song, Appl. Sci. Converg. Technol. 24 (5) (2015) 156–161.
[31] S.N. Walck, T.L. Reinecke, Phys. Rev. B 57 (1998) 9088.
[32] B. Han, C. Robert, E. Courtade, et al., Phys. Rev. X 8 (2018) 031073.
[33] J. Zipfel, J. Holler, A.A. Mitioglu, et al., Phys. Rev. B 98 (2018) 075438.
[34] D. l, W. Kidd, D.K. Zhang, K. Varga, Phys. Rev. B 93 (2016) 125423.
[35] M.Z. Mayers, T.C. Berkelbach, M.S. Hybertsen, D.R. Reichman, Phys. Rev. B 92 (2015) 161404(R).
[36] T. Goldstein, Y.C. Wu, S.Y. Chen, et al., Ground and excited exciton polarons in monolayer $MoSe_2$, arXiv:2005.05829 [cond-mat.mes-hall].
[37] C. Robert, M.A. Semina, F. Cadiz, et al., Phys. Rev. Mater. 2 (2018) 011001(R).
[38] E. Liu, J. Baren, Z. Lu, T. Taniguchi, et al., Gate-tunable exciton-polaron Rydberg series with strong roton effect, arXiv:2006.04895.
[39] A. Arora, T. Deilmann, T. Reichenauer, J. Kern, et al., Phys. Rev. Lett. 123 (2019) 167401.
[40] H. Herold, H. Ruder, G. Wunner, J. Phys. B, At. Mol. Phys. 14 (4) (1981).
[41] M.N. Brunetti, O.L. Berman, R.Ya. Kezerashvilli, J. Phys. Condens. Matter 30 (22) (2018) 225001.
[42] K.J. Nash, M.S. Skolnick, P.A. Claxton, J.S. Roberts, Phys. Rev. B 39 (1989) 10943.
[43] I. Kylänpää, H.-P. Komsa, Phys. Rev. B 92 (2015) 205418.
[44] M.R. Molas, A.O. Slobodeniuk, K. Nogajewski, M. Bartos, et al., Phys. Rev. Lett. 123 (2019) 136801.
[45] O.L. Berman, R.Ya. Kezerashvili, Phys. Rev. B 96 (2017) 094502.
[46] M.M. Fogler, L.V. Butov, K.S. Novoselov, Nat. Commun. 5 (2014) 4555.
[47] A. Steinhoff, M. Florian, M. Rösner, et al., Nat. Commun. 8 (2017) 1166.
[48] K. He, N. Kumar, L. Zhao, et al., Phys. Rev. Lett. 113 (2014) 026803.
[49] P. Steinleitner, P. Merkl, P. Nagler, et al., Nano Lett. 17 (3) (2017) 1455–1460.
[50] F. Xia, H. Wang, D. Xiao, et al., Nat. Photonics 8 (2014) 899–907.
[51] H.P. Komsa, A.V. Krasheninnikov, Phys. Rev. B 86 (2012) 241201(R).
[52] T. Stroucken, J. Neuhaus, S.W. Koch, Mass renormalization in transition metal dichalcogenides, arXiv:2006.03037 [cond-mat.mes-hall].